Conclusions

We have observed—perhaps for the first time—a *ternary* equilibrium of an organolithium compound in THF. CCpLi (**2**) exists as an exo monomer **10**, as an endo monomer **11**, and as an endo,endo dimer **12** in THF at −107 °C. For a 0.34 M solution, the molar ratio of **10**:**11**:**12** is 57:21:22. Approximately the same isomer composition is deduced from time-averaged ^{13}C chemical shifts to persist at room temperature. In the ^{6}Li NMR spectrum of CCpLi (**2**) magnetic anisotropy leads to unusual upfield chemical shifts. This was observed earlier for isodiCpLi (**1**).[4] Two-dimensional $^{6}Li,^{1}H$ HOESY confirms the location of lithium in the individual isomers.

Semiempirical MNDO calculations are in good agreement with the NMR results. The unexpected preference for the exo location of lithium in the monomer is indicated by MNDO to be due to favorable agostic Li–H interactions. These involve the protons of the syn methyl group of the methano bridge in **2**.

That endo quenching products are predominantly found in reactions of CCpLi (**2**) must be a consequence of steric hindrance. While species **10** and **12** of the organolithium reagent might lead to exo products, endo monomer **11** is assumed to be the most reactive species. This may be a consequence of the directing effect of lithium; attachment of the quenching reagent to lithium at the endo face might be preferred energetically in the reaction transition states.

Experimental Section

All experiments were performed in flame-dried glassware under an atmosphere of dry argon.

Synthesis of [(1*R*,7*S*)-1,10,10-Trimethyltricyclo[5.2.1.0^{2,6}]deca-2,5-dien-3-yl]lithium (2). From a solution of diene **9** in diethyl ether the solvent was removed in vacuo. The remaining procedure followed that described in ref 3 by using ^{6}Li-enriched *n*-butyllithium.[5a]

NMR spectra were recorded on a JEOL GX400 spectrometer (9.4 T; ^{1}H, 400 MHz). ^{1}H and ^{13}C NMR spectra are referenced to the signals of the deuterated solvent. THF-d_8: ^{1}H, residual α-H, δ = 3.58 ppm; ^{13}C, α-C, δ = 67.4 ppm. ^{6}Li spectra are referenced to 1 M LiBr in THF/THF-d_8. The reference measurements were carried out prior to the sample measurements at the indicated temperatures.

Spectral Parameters of 2D NMR Spectra.[6] **C,H Shift Correlation (Figure 1)**: A 0.34 M solution of THF-d_8, −107 °C. 90° pulse widths: 9 μs (^{13}C) and 15 μs (^{1}H). Spectral widths: 12723 Hz (^{13}C, f_2) and 2517 Hz (^{1}H, f_1). 4096 data points in t_2, zero filled to 8192 data points. 128 increments in t_1, 64 scans per t_1 increment, Gaussian window in t_1 and t_2. **ROESY (Figure 2)**: A 0.34 M solution in THF-d_8, −107 °C. 90° pulse width: 36 μs (attenuated). Spectral width: 2518 Hz. 1024 data points in t_2, 128 increments in t_1, zero filled to 256 data points. 32 sancs per t_1 increment. Spin lock time: 250 ms [repetitive sequence (12 μs pulse–120 μs delay)$_{320}$; cf. ref 16]. Exponential weighting in t_1 and t_2. **$^{6}Li,^{1}H$ HOESY (Figure 3)**: A 0.34 M solution in THF-d_8, −107 °C. 90° pulse widths: 23 μs (^{6}Li) and 26 μs (^{1}H). Spectral widths: 1200 Hz (^{6}Li, f_2) and 2518 Hz (^{1}H, f_1). 512 data points in f_2, 48 increments in t_1, zero filled to 256 data points. 64 scans per t_1 increments. Gaussian weighting in t_1 and t_2. Pure absorption quadrature detection in f_1.[17]

MNDO calculations were carried out on a CONVEX C210 computer by using the VAMP4 (vectorized AMPAC) software package.[18] All geometry optimizations involved the keyword PRECISE.[19]

Acknowledgment. We thank T. Clark for the vectorized AMPAC program (VAMP4). Financial support by the Deutsche Forschungsgemeinschaft, the Fonds der Chemischen Industrie, the Stiftung Volkswagenwerk, and the National Institutes of Health (Grant CA-12115) is gratefully acknowledged. G.A.O. thanks the U.S. Department of Education for a National Needs Fellowship.

(16) Kessler, H.; Griesinger, C.; Kerssebaum, R.; Wagner, K.; Ernst, R. R. *J. Am. Chem. Soc.* **1987**, *109*, 607.
(17) States, D. J.; Haberkorn, R. A.; Ruben, D. J. *J. Magn. Reson.* **1982**, *48*, 286.
(18) The Dewar Research Group and J. J. P. Stewart, Quantum Chemistry Program Exchange, No. 506, 1986.
(19) Clark, T. *A Handbook of Computational Chemistry*; Wiley: New York, 1985.

^{29}Si Magic-Angle-Spinning NMR Spectroscopy Quantitatively Monitors the Double-Chain/Triple-Chain Intergrowths in Hydrous Silicates

João Rocha,[†] Mark D. Welch,[‡] and Jacek Klinowski*,[†]

Contribution from the Department of Chemistry, University of Cambridge, Lensfield Road, Cambridge CB2 1EW, U.K., and the Department of Earth Sciences, University of Cambridge, Downing Street, Cambridge CB2 3EQ, U.K. *Received March 8, 1991*

Abstract: Stacking phenomena play a central role in the kinetics of many mineral transformations, and quantitative determination of stacking sequences is therefore of major importance. The application of equilibrium thermodynamics to petrological problems depends on the correct interpretation of the thermodynamic status of the various regular and disordered stacking variants. Determination of the proportions of different polysome sequences (e.g. the ratio of double-chain to triple-chain silicates in an intergrowth) is essential to any thermodynamic study of polytypic/polysomatic transformations and disequilibrium time–temperature–transformation studies, from which the cooling histories of metamorphic rocks can be deduced. Although crystal intergrowths can often be imaged by high-resolution transmission electron microscopy, the technique is not suitable for the quantitative determination of polysome proportions. We have examined a polysomatic intergrowth of sodium clinojimthompsonite (hydrous triple-chain structure) and a chemically equivalent sodic amphibole (hydrous double-chain structure) and report that ^{29}Si magic-angle-spinning (MAS) NMR spectroscopy enables the populations of double- and triple-chain silicates in fine-scale lamellar intergrowths of the two polymorphs to be quantitatively determined.

The biopyriboles[1-3] are a family of chain silicates of major petrological interest. The family includes the pyroxenes (single-chain), amphiboles (hydrous double-chain), hydrous triple-chain silicates, and micas (hydrous sheet structures). They form a polysomatic series with pyroxene and mica end-members, denoted by MTO_3 and $AM_3T_4O_{10}(OH)_2$, respectively (A = interlayer site in micas, M = 6- and 8-coordinated atoms, T = tetrahedral atoms). The polysomatic behavior of the series can be considered in terms of the stacking of pyroxene and mica to form

[†] Department of Chemistry.
[‡] Department of Earth Sciences.

(1) Veblen, D. R.; Buseck, P. R.; Burnham, C. W. *Science* **1977**, *198*, 359-365.
(2) Thompson, J. B. *Min. Soc. Am. Rev. Min.* **1981**, *9A*, 141-186.
(3) Veblen, D. R.; Burnham, C. W. *Am. Mineral.* **1978**, *63*, 1053-1073.

0002-7863/91/1513-7100$02.50/0

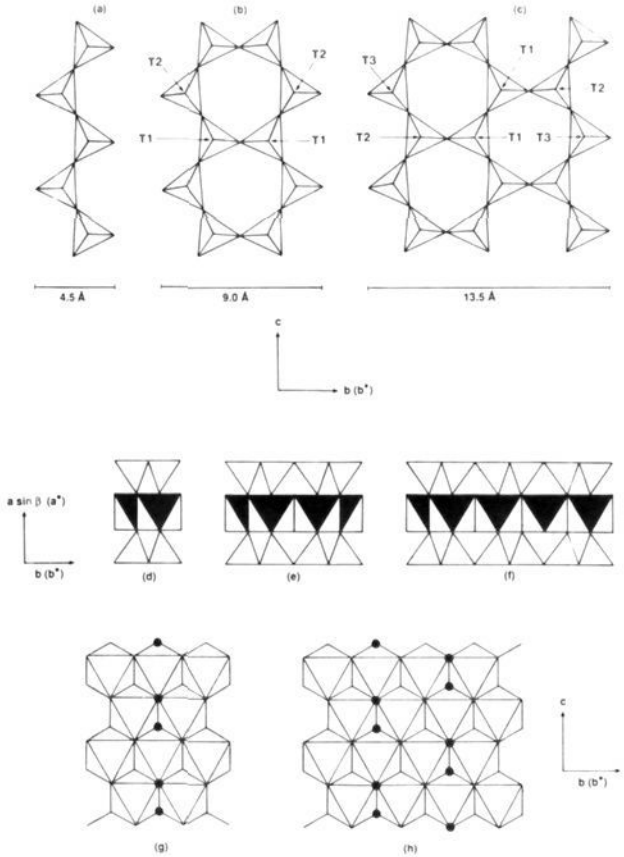

Figure 1. Silicate chains formed by sharing SiO_4 tetrahedra in biopyriboles: (a) single-chain (clinopyroxenes), (b) double-chain (clinoamphiboles), (c) triple-chain silicates. Crystallographic orientation is shown by arrows. The indicated chain widths are $0.5b$. The tetrahedral sites are labeled in the next-nearest-neighbor notation (see text). (d–f) The interlayer octahedral ribbons corresponding to structures a–c. Viewing direction is along c. (g, h) Parts of the octahedral ribbons of the sodic amphibole and SJT, respectively, showing the typical distribution of OH sites (solid circles) in triple-chain and amphibole structures. Structures a–f are adapted from ref 1.

a series of hybrid structures, or polysomes, along the b axis of biopyriboles (which is parallel to b^*). The structures of the single-, double-, and triple-chain biopyriboles are shown schematically in Figure 1. We have examined an intergrowth of triple- and double-chain silicates in the synthetic system Na_2O–MgO–SiO_2–H_2O,[4] with the composition $Na_2O{\cdot}4MgO{\cdot}6SiO_2{\cdot}H_2O$.[5] The reaction is

$$\underset{\text{"sodium clinojimthompsonite" (SJT)}}{4Na_2Mg_4Si_6O_{16}(OH)_2} \rightarrow \underset{\text{amphibole}}{3Na_{2.67}Mg_{5.33}Si_8O_{21.33}(OH)_{2.67}}$$

SJT and amphibole were synthesized hydrothermally from a gel of the composition $Na_2O{\cdot}4MgO{\cdot}6SiO_2$ at 1.7 kbar and 456 °C for 5 days and 1.8 kbar and 700 °C for 3 days, respectively. A lamellar intergrowth of the two polymorphs was prepared at 2 kbar and 653 °C for 3 days. Optical microscopy, X-ray diffraction, high-resolution transmission electron microscopy (HRTEM), and scanning electron microscopy (SEM) indicate that all three products are 100% biopyribole. No amorphous material was found in any of the samples. Electron microprobe analysis (wavelength-dispersive spectrometry) confirms that the biopyriboles have the nominal composition $Na_2O{\cdot}4MgO{\cdot}6SiO_2$. Water contents were determined by hydrogen extraction under vacuum with use of a radio frequency induction heater at 1450 °C to decompose the samples.[6] The water contents are within 7% and 5% relative of the ideal amounts for SJT and amphibole, respectively.

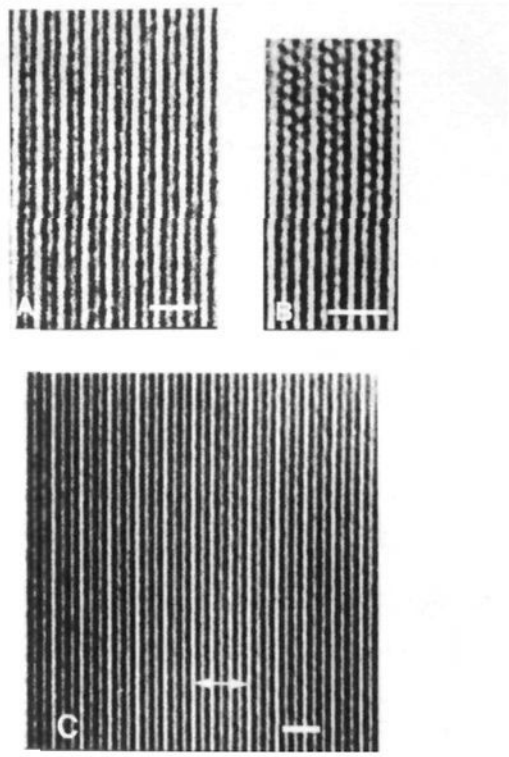

Figure 2. High-resolution electron micrographs of (A) sodic amphibole, (B) SJT, and (C) a lamella of amphibole three double chains wide (27 Å) within a SJT-rich region of a triple–double intergrowth. Viewing direction is [100]. Note that, because of the possible "up" and "down" disposition of the silicate tetrahedra, the unit cell contains *two* chains in the b direction (compare Figure 1, a–c). In all three micrographs the pseudohexagonal "holes" of the Si_6O_{12} rings are seen as either distinct subcircular spots (in SJT) or as diffuse "beaded" strips running parallel to the c axis (amphibole and intergrowth), depending upon focus and contrast. The regions of relatively low electron density associated with the M(5) (SJT) and M(4) (amphibole) strips parallel to (010) appear as "clean" bright stripes. The chain multiplicity (double or triple) is most easily picked out by the latter. A lamella of double-chain structure, three double chains wide, is indicated by a double-headed arrow. All scale bars are 20 Å.

HRTEM (direct lattice imaging and selected area diffraction patterns, SADPs) shows the following: (a) both polymorphs are monoclinic; (b) SADPs are *consistent* with the space groups $C2/m$ for amphibole and $C2/c$ for SJT (the latter is consistent with previous studies of monoclinic triple-chain silicates[4,5]); (c) the two polymorphs have no chain-multiplicity (chain-width) or chain-arrangement (monoclinic/orthorhombic stacking) faults; (d) the intergrowth phase consists predominantly of lamellae of double- and triple-chain structures tens of unit cells wide, with occasional very narrow double-chain lamellae a few unit cells wide (see Figure 2C); (e) microstructures with chain multiplicities other than two or three are absent; and (f) SADPs of the lamellar intergrowth are superpositions of the constituent diffraction patterns of amphibole and SJT, with only very slight streaking parallel to the b module stacking direction, arising from the thinness of lamellae rather than from fine-scale polysomatic disorder.

We conclude that our samples are stoichiometric and have simple microstructures consisting of double- and/or triple-chain elements. Fine-scale chain-width disorder, such as has been observed in some natural amphiboles,[3] is not present. The absence of streaking parallel to b^* in SADPs of the intergrowth confirms its simple two-component lamellar nature and the absence of

(4) Drits, V. A.; Goncharov, Y. I.; Aleksandrova, V. A.; Kladzki, V. E.; Dmitrik, A. L. *Kristallografiya* **1974**, *19*, 737–741.
(5) Tateyama, H.; Shimoda, S.; Sudo, T. *Contrib. Mineral. Petrol.* **1978**, *66*, 149–156.
(6) Holdaway, M. J.; Dutrow, B. L.; Borthwick, J.; Shore, P.; Harmon, R. S.; Hinton, R. W. *Am. Mineral.* **1986**, *71*, 1135–1141.

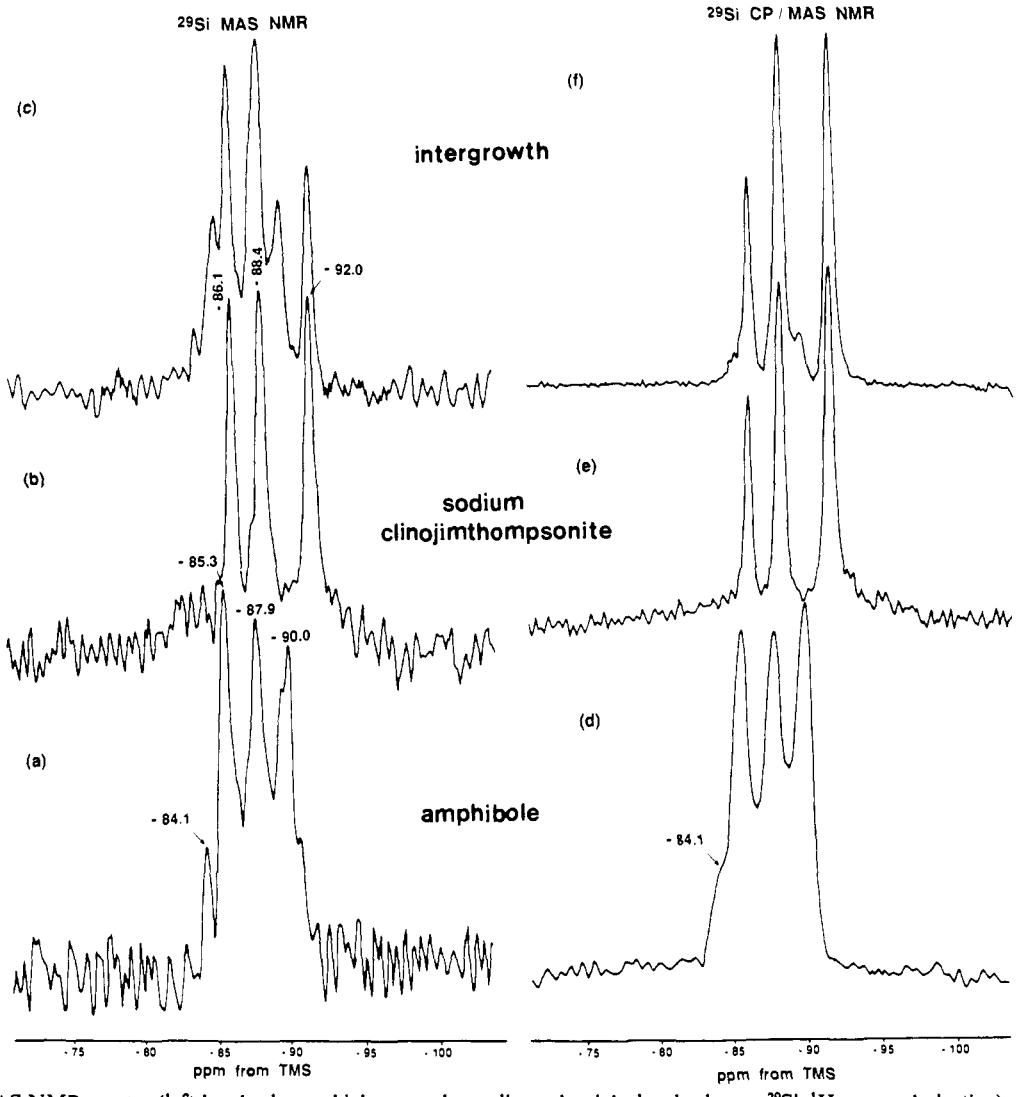

Figure 3. ^{29}Si MAS NMR spectra (left-hand column: high-power decoupling only; right-hand column: $^{29}Si-^{1}H$ cross-polarization) of (a, d) amphibole, (b, e) triple-chain (SJT) silicate, and (c, f) a lamellar intergrowth of double- and triple-chain silicates. MAS NMR spectra were acquired with 4.0 μs radio frequency pulses (equivalent to 48° pulse angle). Because of the long ^{29}Si spin-lattice relaxation times, recycle delays of 300 s (b and c) and 900 s (a) were used in order to avoid saturation effects (see text). CP/MAS spectra were acquired with (e and f) 8-s and (d) 20-s recycle delays (due to the long proton T_1 of the amphibole), a 10-ms contact time, and 7.5-μs proton 90° pulses.

fine-scale polysomatic disorder.

The proportion of double- and triple-chain structures in an intergrowth cannot be accurately determined by X-ray diffraction (XRD), principally because of the considerable dependence of the width of XRD peaks on particle size. This is particularly serious in the case of SJT-rich intergrowths, which grow only at relatively low temperatures (450–550 °C). The microcrystals of these are less than 1 μm in diameter (M. D. Welch, unpublished work). With regard to HRTEM as a quantitative tool, the (010)-fringe counting method[7,8] assumes that chain-multiplicity faults (polysomatic stacking errors) observed in *b–c* direct-lattice images extend throughout the crystal in the third dimension, so that two-dimensional fringe counting is entirely representative of the bulk crystal. However, it has been shown[9] that chain-multiplicity faults are often discontinuous in the third dimension (*a* axis). Furthermore, the fringe-counting method is extremely slow and tedious (involving counting ca. 2500 subchains per sample). MAS NMR, which monitors *local* order in the bulk sample, does not suffer from the limitations of XRD and HRTEM. We will see that ^{29}Si MAS NMR signals from SJT are in fact narrower than those from the amphibole.

The structure of SJT[5] has three distinct Si environments, Q^2, Q^{3a}, and Q^{3b}, present in the 1:1:1 population ratio (see Figure 2C):

SJT	Q^3-Si-$(Q^3)_2$	Q^3-Si-$(Q^2)_2$	Q^3-Si-Q^3
	Q^{3a} (T1)	Q^{3b} (T2)	Q^2 (T3)

where Q denotes a tetrahedrally coordinated Si site linked to two (Q^2) or three (Q^3) other tetrahedral Si. This should correspond to three signals of equal intensity in the ^{29}Si MAS NMR spectrum. The amphibole has an unusual stoichiometry in that it contains 0.67 H atom per formula in excess of the usual 2 H atoms. A similar amphibole containing Li instead of Na has been synthesized.[10] It has the formula $Li_{1.38}Mg_{5.89}Si_{8.01}O_{21.20}(OH)_{2.80}$ and contains 0.8 excess H atom.

All amphiboles have a Q^2:Q^3 ratio of 1:1, and so any interpretation of their spectra must fulfil this requirement. For example, *C*2/*m* tremolite has three signals: two Q^2 of equal intensity, and a single Q^3 twice the intensity of Q^2 signals.[11] However, as will be seen later, the ideal Q^2:Q^3 ratio is not easily deduced from the spectrum of our unusual amphibole. The tentative assignment of *C*2/*m* symmetry for the amphibole and the absence of superlattice reflections in electron diffraction patterns may imply

(7) Maresch, W. V.; Czank, M. *Period. Mineral. (Rome)* **1983**, *52*, 463–542.
(8) Maresch, W. V.; Czank, M. *Fortschr. Mineral.* **1988**, *66*, 69–121.
(9) Veblen, D. R.; Buseck, P. R. *Am. Mineral.* **1979**, *64*, 687–700.
(10) Maresch, W. V.; Langer, K. *Contrib. Mineral. Petrol.* **1976**, *56*, 27–34.
(11) Mägi, M.; Lippmaa, E.; Samoson, A.; Engelhardt, G.; Grimmer, A.-R. *J. Phys. Chem.* **1984**, *88*, 1518–1522.

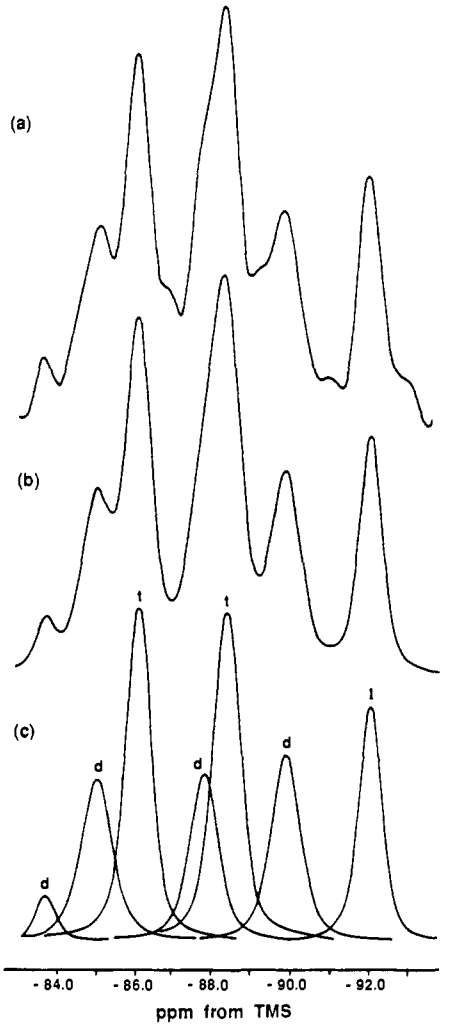

Figure 4. The ^{29}Si MAS NMR spectrum of a lamellar intergrowth of double- and triple-chain silicates is a superposition of the individual spectra of double- and triple-chain structures. Spectral deconvolution allows the relative amounts of the latter phases to be quantified as 42 ± 5 and 58 ± 5 mol %, respectively. (a) Experimental spectrum, (b) simulated spectrum, (c) individual resonances used in the simulation. "d" and "t" refer to NMR signals assigned to silicon atoms in double and triple chains, respectively.

disordering of Na and Mg atoms over the M(4) sites. As yet the distribution of the excess H atoms in the structure of our amphibole is unknown and, consequently, it is not possible at present to offer a model for the comprehensive interpretation of the NMR spectrum. However, this has no bearing upon the determination of the *proportions* of double and triple chains, because, as we show below, the spectrum of the intergrowth is a simple superposition of the spectra of the two component materials.

^{29}Si MAS spectra were acquired at 79.5 MHz on a Bruker MSL-400 spectrometer with use of high-power proton decoupling. ^{29}Si–^{1}H cross-polarization (CP/MAS) experiments were carried out to investigate the status of the hydrogen in the samples. CP/MAS experiments were carried out with single contacts and contact times of between 500 μs and 150 ms. The Hartmann–Hahn condition was set with a sample of kaolinite.[12] The rotors were spun in air at 4.5 kHz in a double-bearing probehead. Chemical shifts are quoted in ppm from external TMS.

The NMR spectra are given in Figure 3. All are well resolved and, given the very long ^{29}Si spin–lattice relaxation times in these compact structures (we estimate that for amphibole $T_1 \approx 900$ s), have a good signal-to-noise ratio. However, the ^{29}Si relaxation times of the amphibole intergrowth are shorter than those of pure amphibole. Amphibole gives four signals centered at −90.0, −87.9, −85.3, and −84.1 ppm. The spectra of SJT consist of narrow resonances at −92.0, −88.4, and −86.1 ppm with half-widths of 50–70 Hz (Figure 3b). Five resonances at −91.9, −89.9, −88.3, −86.0, and −85.0 ppm (with a possible sixth at ca. −84 ppm) are resolved in the spectrum of the double-chain/triple-chain intergrowth. Moreover, the signal at −88.3 ppm has a shoulder at ca. −87.9 ppm (best seen in the expansion in Figure 4c).

It is clear from Figure 3 that the spectrum of the lamellar intergrowth is explicitly a superposition of the individual spectra of the double- and triple-chain silicates. NMR spectral intensity (the area under a peak) is proportional to the number of ^{29}Si nuclei in the sample provided that the recycle delay used takes into account the *longest* relaxation time. Since we were very careful to do this, the relative amounts of the two structures in the intergrowth can be quantified by simple deconvolution of the spectrum given in Figure 3c. Such line simulation for our particular intergrowth is shown in Figure 4, giving the relative amounts of the double- and triple-chain polymorphs as 42 ± 5 and 58 ± 5 mol %, respectively. We note that the NMR resonances of the lamellar intergrowth are narrower than those given by either pure polymorph. This is probably due to a higher degree of local order around the double-chain/triple-chain Si tetrahedra.

The two SJT resonances at −92.0 and −88.4 ppm are assigned to Q^{3b} and Q^{3a} sites, respectively. This assignment is based on bond-angle/bond-length data for clinojimthompsonite,[3] the Q^{3a} sites having a longer average bond length and a smaller average bond angle than the Q^{3b} sites. One would therefore expect[13] the Q^{3a} resonance to be shifted to low field relative to the Q^{3b} resonance. The resonance at −86.1 ppm is assigned to the Q^2 site. The Q^3/Q^2 ratio of ca. 2 obtained by spectral deconvolution fully agrees with the model proposed above.

Spectral deconvolution of the amphibole spectrum gives the ratio of 1:1:1:0.2 for the relative intensities of the −90.0 to −84.1 ppm resonances. An examination of the change in the CP/MAS spectrum of the amphibole as a function of contact time (not shown) reveals an enhancement of the −85.3-ppm resonance for short contact times, due to shorter T_{Si-H} relaxation time. This suggests that this resonance is due to $Q^2(OH)$. A similar enhancement of the resonance at −87.9 ppm is observed for long contact times, suggesting that the corresponding Si site has the longest Si–H distance. The resonance at −84.1 ppm is difficult to assign, but it corresponds to a Si site that relaxes more slowly than the other three Si sites.

It is clear that solid-state NMR spectroscopy is a powerful tool not only for the determination of Si, Al ordering in zeolites[14,15] and minerals[16,17] but also for the quantification of geologically important fine-scale polysomatic phenomena in silicates. When combined with disequilibrium time–temperature–transformation studies, NMR spectroscopy could enable the heating/cooling histories of metamorphic rocks to be established.

Acknowledgment. We are grateful to ECC International Limited, Shell Research, Amsterdam, and the University of Aveiro for support. M.D.W. thanks the NERC for a Special Research Fellowship.

Registry No. $NaMg_2Si_3O_8(OH)$, 135393-28-1; $Mg_{5.33}Na_{2.67}Si_8O_{21.33}(OH)$, 135426-01-6.

(12) Rocha, J.; Klinowski, J. *J. Magn. Reson.* **1990**, *90*, 567–568.
(13) Engelhardt, G.; Michel, D. *High-resolution Solid-state NMR of Silicates and Zeolites*; John Wiley & Sons: New York, 1987.
(14) Klinowski, J.; Ramdas, S.; Thomas, J. M.; Fyfe, C. A.; Hartman, J. S. *J. Chem. Soc., Faraday Trans. II* **1982**, *78*, 1025–1050.
(15) Fyfe, C. A.; Gobbi, G. C.; Klinowski, J.; Thomas, J. M.; Ramdas, S. *Nature* **1982**, *296*, 530–533.
(16) Fyfe, C. A.; Gobbi, G. C.; Klinowski, J.; Putnis, A.; Thomas, J. M. *J. Chem. Soc., Chem. Commun.* **1983**, 556–558.
(17) Klinowski, J.; Carr, S. W.; Tarling, S. E.; Barnes, P. *Nature* **1987**, *330*, 56–58.